N/O- and C-Bound (Enolato)palladium Complexes with Hydrotris(pyrazolyl)borato Ligands (Tp^R: R = iPr_2, Me_2) Obtained via Dehydrative Condensation between the Hydroxo Complexes $Tp^RPd(Py)OH$ and Active Methylene Compounds: Factors Determining the Isomer Distribution and Dimerization of Cyano Compounds

Masato Kujime, Shiro Hikichi, and Munetaka Akita*

Chemical Resources Laboratory, Tokyo Institute of Technology, 4259 Nagatsuta, Midori-ku, Yokohama 226-8503, Japan

Received May 29, 2001

Reaction of a hydroxopalladium complex bearing the Tp^{iPr_2} ligand, $(Tp^{iPr_2})(py)Pd-OH$ (**1^{iPr_2}**), with active methylene compounds, $X-CH_2-Y$ **2** [dicyanomethane (**2a**), methyl cyanoacetate (**2b**), benzoylacetonitrile (**2c**)], resulted in dehydrative condensation to afford the N/O-bound enolates, $(Tp^{iPr_2})(py)Pd-X-CH-Y$ **3^{iPr_2}a−c**. When the hydroxo complex **1^{Me_2}** with the less bulky Tp^{Me_2} ligand was allowed to react with **2** at 0 °C, similar N/O-bound enolato complexes, $(Tp^{Me_2})(py)Pd-X-CH-Y$ (**3^{Me_2}a−c**), were obtained as kinetic products, which were gradually converted to the more stable C-bound enolato complexes $(Tp^{Me_2})(py)Pd-CHXY$ (**4^{Me_2}a−c**) upon warming to 50 °C. X-ray crystallography of the N/O- and C-bound enolates reveals that (1) the Pd center adopts the square-planar or square-pyramidal geometry, (2) the structure of the C-bound isomer is consistent with the canonical structure with the localized bonding scheme, and (3) in the N/O-bound isomers the negative charge is delocalized over the X−CH−Y linkage to form the zwitterionic structure. The N-bound enolato complexes **3a**,**b** obtained from cyano compounds further reacted with the cyano compounds to give the 1:2 condensates: i.e., the 2-cyanoethenylamido complexes $(Tp^R)(py)Pd-NH-C(CH_2Y)=CCN-(Y)$ (**6**), whereas the C-bound enolates **4^{Me_2}a,b** showed no indication of the dimerization. Thus, the present study reveals that the reactivity of transition-metal enolates is dependent on their structures.

Introduction

Transition-metal enolates[1] are expected to display chemical reactivity which has not been realized by main-group-metal enolates.[2] For example, unsaturated hydrocarbons and aromatic halides have a chance to be coupled with enolates. In particular, the recent reports by Murahashi on Ru-catalyzed aldol and Michael reactions have attracted much attention, because the dehydrative condensation was effected via C−H activation under neutral reaction conditions.[3,4] It was also demonstrated that reactant selectivity is not dependent on the acidity of the C−H moiety to be activated but on the kind of the functional groups included in the molecule.

As an extension of the chemistry of Tp^RM complexes (Tp^R = hydrotris(pyrazolyl)borato ligands)[5] to organometallic systems[6,7] (e.g. highly coordinatively unsatur-

(1) (a) Heathcock, C. H. In *Comprehensive Organic Synthesis*; Trost, B. M., Ed.; Pergamon: Oxford, U.K., 1991; Vol. 2, Chapter 1.9. (b) Burkhardt, E. R.; Doney, J. J.; Slough, G. A.; Stack, J. M.; Heathcock, C. H.; Bergman, R. G. *Pure Appl. Chem.* **1988**, *60*, 1. (c) Davies, S. G. *Pure Appl. Chem.* **1988**, *60*, 13. (d) Brunner, H. *Angew. Chem., Int. Ed.* **1999**, *38*, 1194. (e) Slough, G. A.; Bergman, R. G.; Heathcock, C. H. *J. Am. Chem. Soc.* **1989**, *111*, 938. (f) Burkhardt, E. R.; Bergman, R. G.; Heathcock, C. H. *Organometallics* **1990**, *9*, 30. (g) Stack, J. G.; Doney, J. J.; Bergman, R. G.; Heathcock, C. H. *Organometallics* **1990**, *9*, 453. (h) Hartwig, J. F.; Andersen, R. A.; Bergman, R. G. *Organometallics* **1991**, *10*, 3326. (i) Hartwig, J. F.; Bergman, R. G.; Andersen, R. A. *Organometallics* **1991**, *10*, 3344. (j) Balegroune, F.; Grand-jean, D.; Lakkis, D.; Matt, D. *J. Chem. Soc., Chem. Commun.* **1992**, 1084. (k) Veya, P.; Floriani, C.; Chiesi-Villa, A.; Rizzoli, C. *Organometallics* **1993**, *12*, 4892. (l) Veya, P.; Floriani, C.; Chiesi-Villa, A.; Rizzori, C. *Organometallics* **1993**, *12*, 4899. (m) Hamann, B. C.; Hartwig, J. F. *J. Am. Chem. Soc.* **1997**, *119*, 12382. (n) Fujii, A.; Hagiwara, E.; Sodeoka, M. *J. Am. Chem. Soc.* **1999**, *121*, 5450. (o) Ruiz, J.; Rodríguez, V.; Cutillas, N.; Pardo, M.; Pérez, J.; López, G.; Chaloner, P.; Hitchcock, P. B. *Organometallics* **2001**, *20*, 1973. (p) Vicente, J.; Arcas, A.; Fernández-Hernández, J. M.; Bautista, D. *Organometallics* **2001**, *20*, 2767. (q) Culkin, D. A.; Hartwig, J. F. *J. Am. Chem. Soc.* **2001**, *123*, 5816.

(2) (a) *Comprehensive Organic Synthesis*; Fleming, I., Trost, B. M., Eds.; Pergamon: Oxford, U.K., 1991; Vols. 2 and 3. (b) Seebach, D. *Angew. Chem., Int. Ed. Engl.* **1988**, *27*, 1624. (c) Smith, M. B.; March, J. *Advanced Organic Chemistry*, 5th ed.; Wiley-Interscience: New York, 2001.

(3) (a) Naota, T.; Taki, H.; Mizuno, M.; Murahashi, S.-I. *J. Am. Chem. Soc.* **1989**, *111*, 5954. (b) Murahashi, S.-I.; Naota, T.; Taki, H.; Mizuno, M.; Takaya, H.; Komiya, S.; Mizuho, Y.; Oyasato, N.; Hiraoka, M.; Hirano, M.; Fukuoka, A. *J. Am. Chem. Soc.* **1995**, *117*, 12436. (c) Takaya, H.; Naota, T.; Murahashi, S.-I. *J. Am. Chem. Soc.* **1998**, *120*, 4244. (d) Naota, T.; Tannna, A.; Murahashi, S.-I. *J. Am. Chem. Soc.* **2000**, *122*, 2960. (e) Murahashi, S.-I.; Take, K.; Naota, T.; Takaya, H. *Synlett* **2000**, 1016. (f) Murahashi, S.-I.; Naota, T. *Bull. Chem. Soc. Jpn.* **1996**, *69*, 1805. (g) Murahashi, S.; Takaya, H. *Acc. Chem. Res.* **2000**, *33*, 225.

(4) (a) Mizuho, Y.; Kasuga, N.; Komiya, S. *Chem. Lett.* **1991**, 2127. (b) Hirano, M.; Ito, Y.; Hirai, M.; Fukuoka, A.; Komiya, S. *Chem. Lett.* **1993**, 2057. (c) Hirano, M.; Hirai, M.; Ito, Y.; Tsurumaki, T.; Baba, A.; Fukuoka, A.; Komiya, S. *J. Organomet. Chem.* **1998**, *569*, 3. (d) Hirano, M.; Takenaka, A.; Mizuho, Y.; Hiraoka, M.; Komiya, S. *J. Chem. Soc., Dalton Trans.* **1999**, 3209.

10.1021/om010448o CCC: $20.00
Publication on Web 08/16/2001

ated hydrocarbyl complexes, Tp^RM-R', M = Fe (14e), Co (15e)),[6b,g,o] we examined the synthesis and reactivity of (enolato)palladium complexes as an example of functionalized alkyl complexes. Transition-metal enolates studied extensively for the last two decades[1,3,4] have been prepared mainly by three methods: (1) dehydrative condensation between a transition-metal hydroxide and carbonyl compounds, (2) a metathesis reaction between a transition-metal halide and main-group-metal enolates, and (3) oxidative addition of a β-oxoalkyl halide to a low-valent metal species.[8] Because our first attempts to synthesize ketone enolates, $(Tp^R)(py)Pd-CH_2(C{=}O)R'$ or $-OC(R'){=}CH_2$, by reaction of $(Tp^R)(py)Pd-Cl$ (or $[(Tp^R)(py)_2Pd]^+$) with various enolate anions (method 2) were unsuccessful, the substrate was changed to active methylene compounds. Although the metathesis reaction also has not met with success, dehydrative condensation with the hydroxo complex $(Tp^R)(py)Pd-OH$[7a] and active methylene compounds CH_2XY (X, Y= CN, COR) (method 1) successfully produced the expected enolato complexes. Herein we disclose the synthesis, characterization, isomer distribution, and reactivity of N/O- and C-bound (enolato)palladium complexes bearing Tp^R ligands, $(Tp^R)(py)Pd-X-CH-Y$ and $(Tp^R)(py)Pd-CHXY$.

Scheme 1

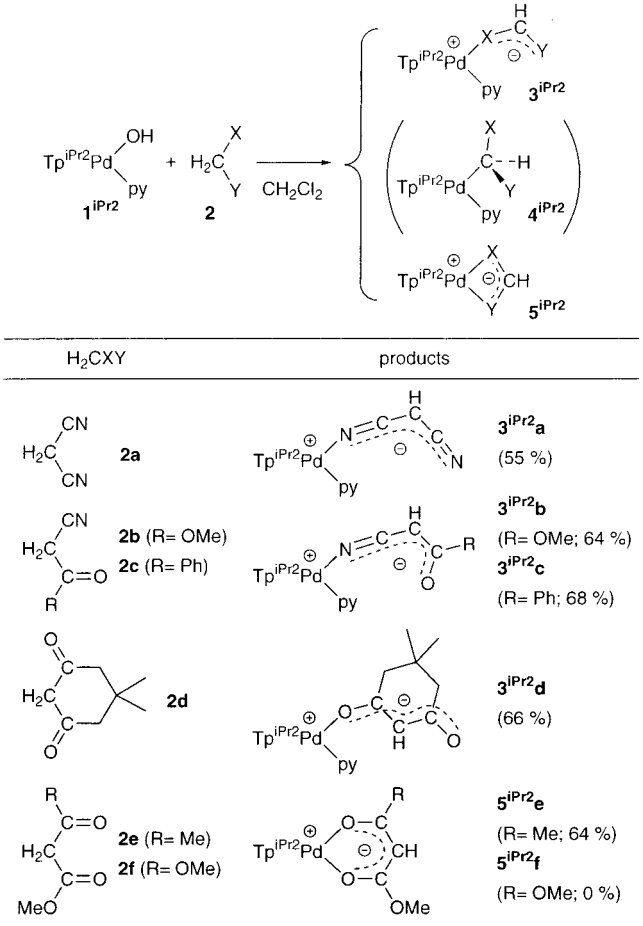

Results

Preparation of $Tp^{iPr_2}Pd(py)-$Enolate Complexes via Dehydrative Condensation of $Tp^{iPr_2}Pd(py)-OH$ (1^{iPr_2}) with Active Methylene Compounds 2 To Give N/O-Bound Enolato Complexes. When active methylene compounds **2** were treated with the hydroxopalladium complex bearing the Tp^{iPr_2} ligand $\mathbf{1^{iPr_2}}$ in the presence of Na_2SO_4, dehydrative condensation proceeded to give yellow to orange complexes $\mathbf{3^{iPr_2}}$ and $\mathbf{5^{iPr_2}}$ as the sole products (Scheme 1).[9]

The products $\mathbf{3^{iPr_2}a-c}$ obtained from cyano compounds show the ν_{CN} and ν_{CO} vibrations, which are shifted to lower energies compared to those of the starting compounds (ν_{CN}, $\mathbf{3^{iPr_2}a-c}$ < 2200 cm^{-1} < **2a–c**; ν_{CO}, $\mathbf{3^{iPr_2}b,c}$ < 1700 cm^{-1} < **2b**,**c**) (Table 1). When the following aspects ((1) the larger $^1J_{CH}$ values for the CH–CN methine carbon atom (>170 Hz) indicative of sp^2 hybridization and (2) the presence of the pyridine ligand) are taken into account,[10] it is suggested that square-planar N/O-bound enolates (rather than C-bound enolates) are formed via the dehydrative reaction. It should be noted that (1) one of the two δ_C(CN) signals observed for $\mathbf{3^{iPr_2}a}$ (δ_C 143.5) is shifted to lower field than the other signal (δ_C 125.2), which appears in the normal range of CN signals, and (2) the δ_C(CN) signals

(5) Abbreviations used in this paper: Tp^R, hydrotris(pyrazolyl)borato ligands; Tp^{iPr_2}, 3,5-diisopropylpyrazolyl derivative; Tp^{Me_2}, 3,5-dimethylpyrazolyl derivative; pz^R, pyrazolyl group in Tp^R; 4-pz-H, hydrogen atom at the 4-position of pz^R; 3-, 4-, and 5-pz, pz ring carbon atoms at 3-, 4-, and 5-positions, respectively. The superscript in the compound number denotes the kind of Tp^R ligand.

(6) Our recent work based on the Tp^R ligand: (a) Akita, M.; Ohta, K.; Takahashi, Y.; Hikichi, S.; Moro-oka, Y. *Organometallics* **1997**, *16*, 4121. (b) Akita, M.; Shirasawa, N.; Hikichi, S.; Moro-oka, Y. *Chem. Commun.* **1998**, 973. (c) Hikichi, S.; Komatsuzaki, H.; Akita, M.; Moro-oka, Y. *J. Am. Chem. Soc.* **1998**, *120*, 4699. (d) Hikichi, S.; Yoshizawa, M.; Sasakura, Y.; Akita, M.; Moro-oka, Y. *J. Am. Chem. Soc.* **1998**, *120*, 10567. (e) Akita, M.; Miyaji, T.; Hikichi, S.; Moro-oka, Y. *Chem. Commun.* **1998**, 1005. (f) Takahashi, Y.; Akita, M.; Hikichi, S.; Moro-oka, Y. *Organometallics* **1998**, *17*, 4884. (g) Shirasawa, N.; Akita, M.; Hikichi, S.; Moro-oka, Y. *Chem. Commun.* **1999**, 417. (h) Takahashi, Y.; Hikichi, S.; Akita, M.; Moro-oka, Y. *Chem. Commun.* **1999**, 1491. (i) Takahashi, Y.; Hikichi, S.; Akita, M.; Moro-oka, Y. *Organometallics* **1999**, *18*, 2571. (j) Ohta, K.; Hashimoto, M.; Takahashi, Y.; Hikichi, S.; Akita, M.; Moro-oka, Y. *Organometallics* **1999**, *18*, 3234. (k) Takahashi, Y.; Hashimoto, M.; Hikichi, S.; Akita, M.; Moro-oka, Y. *Angew. Chem., Int. Ed.* **1999**, *38*, 3074. (l) Akita, M.; Miyaji, T.; Hikichi, S.; Moro-oka, Y. *Chem. Lett.* **1999**, 813. (m) Hikichi, S.; Yoshizawa, M.; Sasakura, Y.; Komatsuzaki, H.; Akita, M.; Moro-oka, Y. *Chem. Lett.* **1999**, 979. (n) Akita, M.; Hashimoto, M.; Hikichi, S.; Moro-oka, Y. *Organometallics* **2000**, *19*, 3744. (o) Shirasawa, N.; Nguyet, T. T.; Hikichi, S.; Moro-oka, Y.; Akita, M. *Organometallics* **2001**, *20*, 3582. Reviews: (p) Akita, M.; Hikichi, S.; Moro-oka, Y. *J. Synth. Org. Chem.* **1999**, *57*, 619. (q) Hikichi, S.; Akita M., Moro-oka, Y. *Coord. Chem. Rev.* **2000**, *198*, 61.

(7) For $Tp^RM(L)-OH$ complexes, see the following references. M = Pd: (a) Akita, M.; Miyaji, T.; Muroga, N.; Mock-Knoblauch, C.; Adam, W.; Hikichi, S.; Moro-oka, Y. *Inorg. Chem.* **2000**, *39*, 2096. M = V: (b) Kosugi, M.; Hikichi, S.; Akita, M.; Moro-oka, Y. *Inorg. Chem.* **1999**, *38*, 2567. (c) Kosugi, M.; Hikichi, S.; Akita, M.; Moro-oka, Y. *J. Chem. Soc., Dalton Trans.* **1999**, 1369. M = Mn: (d) Komatsuzaki, H.; Ichikawa, S.; Hikichi, S.; Akita, M.; Moro-oka, *Inorg. Chem.* **1998**, *37*, 3652. (e) Komatsuzaki, H.; Sakamoto, N.; Satoh, M.; Hikichi, S.; Akita, M.; Moro-oka, Y. *Inorg. Chem.* **1998**, *37*, 6554. (f) Kitajima, N.; Singh, U. P.; Amagai, H.; Osawa, M.; Moro-oka, Y. *J. Am. Chem. Soc.* **1991**, *113*, 7757. M = Fe: (g) Ogihara, T.; Hikichi, S.; Fujisawa, K.; Kitajima, N.; Akita, M.; Moro-oka, Y. *Inorg. Chem.*, **1997**, *36*, 4539. M = Co, Ni: (h) Hikichi, S.; Yoshizawa, M.; Sasakura, Y.; Akita, M.; Moro-oka, Y. *J. Am. Chem. Soc.* **1998**, *120*, 10567. (i) Kitajima, N.; Hikichi, S.; Tanaka, M.; Moro-oka, Y. *J. Am. Chem. Soc.* **1993**, *115*, 5496; Cu: (j) Kitajima, N.; Koda, T.; Hashimoto, S.; Kitagawa, T.; Moro-oka, Y. *J. Am. Chem. Soc.* **1991**, *113*, 5664. M = Ru: (k) Takahashi, Y.; Akita, M.; Hikichi, S.; Moro-oka, Y. *Inorg. Chem.* **1998**, *37*, 3186. (l) Akita, M.; Takahashi, Y.; Hikichi, S.; Moro-oka, Y. *Inorg. Chem.* **2001**, *40*, 169. For other metal complexes see also: (m) Parkin, G. *Adv. Inorg. Chem.* **1995**, *42*, 291.

(8) For Pd complexes, see refs 1l,o and references therein.

(9) When an acetone solution of $\mathbf{1^{iPr_2}}$ was refluxed for several hours, a mixture of products containing $(Tp^{iPr_2})(py)Pd-CH_2C(=O)CH_3$ was obtained but a pure sample could not be isolated from it.

(10) Pretsch, P. D.; Seible, J.; Simon, W.; Clerc, T. *Strukturaufklälung organischer Verbindungen*, 2nd ed.; Springer: Berlin, 1981.

Table 1. Selected Spectroscopic Data for 3−5

compd	IR/cm^{-1} [a] ν_{BH}	IR/cm^{-1} [a] others	^{1}H NMR/δ_H [b−d] 4-pz-H	^{1}H NMR/δ_H [b−d] CH	^{1}H NMR/δ_H [b−d] others	^{13}C NMR/δ_C [c−e] enolate
3^{iPr_2}a	(2545)[f]	2189[g]	5.72	1.96		6.3 (d, J = 180, CH), 125.2 (s, CN), 143.5 (s, Pd−NC)
	2485	2110[g]	5.83			
		1607[h]	5.96			
3^{iPr_2}b[i,j]	2533	2139[g]	5.72	2.92	3.32	34.3, 34.4 (d × 2, J = 173, CH), 49.5, 49.8 (q × 2, J = 144, OMe),
	2482	1646[k]	5.84	2.68	3.37	139.9, 140.5 (s × 2, CN), 173.2. 173.9 (s × 2, C=O)
		1606[h]	5.97			
3^{iPr_2}c	(2545)[f]	2185[g]	5.74	4.29		51.0 (d, J = 169, CH), 136.2 (s, CN), 188.7 (s, C=O)
	2486	1608[h]	5.85			
			5.95			
3^{iPr_2}d	2479	1617[k]	5.72	4.85	0.62	27.9 (q, J = 125, C*Me*$_2$), 32.2 (s, *C*Me$_2$),
			5.82		0.65	47.5, 50.3 (d × 2, J = 126, CH$_2$), 104.0 (d, J = 158, CH),
			6.02			188.5, 197.4 (t × 2, J = 5, C=O)
5^{iPr_2}e	2545	1599[k]	5.75 (1H)	4.79	1.83	25.0 (q, J = 127, CO*Me*), 52.2 (q, J = 146, OMe),
			5.82 (2H)		3.56	84.7 (d, J = 162, CH), 171.0, 186.6 (s × 2, C=O)
3^{Me_2}a[i]	2522	2188[g]	5.69	2.02		6.4 (d, J = 182, CH), 124.2 (s, CH), 144.0 (s, Pd−NC)
	2484	2138[g]	5.81			
		2110[g]	5.85			
		1608[h]				
4^{Me_2}a	2468	2230[g]	5.65	2.72		−15.9 (d, J = 151, Pd−CH), 118.6, 120.5 (d × 2, J = 8, CN)
		2215[g]	5.86			
		1609[h]	5.93			
3^{Me_2}b[i,j]	2516	2170[g]	5.69	2.94	3.32	38.7, 39.3 (d × 2, J = 171, CH), 54.0, 54.4 (q x 2, J = 144, OMe),
		1639[k]	5.79	2.71	3.35	145.4, 146.5 (s × 2, CN), 177.7, 178.3 (s × 2, C=O)
		1607[h]	5.84			
4^{Me_2}b	2473	2206[g]	5.67	3.17	3.11	5.2 (d, J = 147, Pd−CH), 51.5 (q, J = 146, OMe),
		1699[k]	5.87			123.9 (s, CN), 172.5 (d, J = 7 Hz, C=O)
		1608[h]	5.89			
3^{Me_2}c[l]	2512	2191[g]	5.69	4.30		50.0 (d, J = 169, CH), 140.3 (d, J = 7, CN), 186.7 (s, C=O)
		1608[h]	5.81			
			5.86			
4^{Me_2}c	2511	2205[g]	5.11	4.19		14.1 (d, J = 143, Pd−CH), 124.6 (d, J = 6, CN),
		1676[k]	5.58			195.8 (d, J = 4, C=O)
		1609[h]	5.97			
3^{Me_2}d	2474	1611[k]	5.72 (2H)	5.19	0.68	28.1, 28.3 (q, J = 130, C*Me*$_2$), 32.3 (s, *C*Me$_2$),
			5.94 (1H)			47.6, 50.2 (t × 2, J = 125, CH$_2$), 103.8 (d, J = 156, CH),
						188.9, 197.6 (s × 2, C=O)

[a] Observed as KBr pellets. [b] Observed at 400 MHz in $CDCl_3$ at room temperature unless otherwise stated. [c] Multiplicities and coupling constants (in Hz) are shown in parentheses. Signals are singlets unless otherwise stated. [d] Other signals are reported in the Experimental Section. [e] Observed at 100 MHz in $CDCl_3$ at room temperature unless otherwise stated. [f] The weak signals were occasionally observed, depending on the conditions of the samples (see text.). [g] ν_{CN}. [h] ν_{py}. [i] NMR spectra were observed at −50 °C in CD_2Cl_2. [j] A mixture of stereoisomers (see text). [k] ν_{CO}. [l] NMR spectra were observed at −80 °C in CD_2Cl_2.

for **3^{iPr_2}b**,**c** appear in the former region.[10] These observations, similar to those of the N-bound Ru−enolato complexes reported by Murahashi[3] and Komiya,[4] lead to the assignment of **3^{iPr_2}a**−**c** as the N-bound enolates. The N-coordination of **3^{iPr_2}c** derived from benzoylacetonitrile **2c** was confirmed by X-ray crystallography (Figure 1 and Table 2), and the spectroscopic features of **3^{iPr_2}b** are close to those of the N-bound Tp^{Me_2} derivative **3^{Me_2}b**, which was also characterized crystallographically (see below). Structural features will be discussed later. Thus, the enolato complexes derived from cyano compounds turn out to be square-planar N-bound species (**3^{iPr}a**−**c**). López and co-workers reported the closely related dehydrative condensation between the dianionic bis(μ-hydroxo)dipalladium complex $[(C_6F_5)_4Pd_2(\mu\text{-}OH)_2]^{2-}$ and **2a** to give the dinuclear bis(μ-malononitrilate) complex $[(C_6F_5)_4Pd_2[\mu\text{-}CH(CN)\text{-}CN]_2]^{2-}$.[11]

1,3-Diketones also undergo dehydration with **1^{iPr_2}**. Dimedone (**2d**) affords the O-bound enolato complex **3^{iPr}e**, which is characterized by its spectroscopic features ((1) two kinds of δ_C(CO) signals and (2) the presence of the sp^2-hybridized methine carbon signal at δ_C 104.0) similar to those of the above-mentioned N-bound enolato complexes **3^{iPr_2}a**−**c**. In contrast to the hitherto discussed reactions, methyl acetoacetate (**2e**) produces the chelate product **5^{iPr_2}e**, resulting from elimination of the pyridine ligand, but no reaction is observed with dimethyl malonate (**2f**). Formation of similar chelated products was recently reported for the (κ^2-*o*-$C_6H_4CH_2NMe_2$)Pd system having two cis coordination sites.[10]

Thus, the reaction of **1^{iPr_2}** with active methylene compounds containing CN and CO functional groups produces the N/O-bound enolato complexes **3^{iPr_2}** and no indication for formation of the C-bound enolato complex **4^{iPr_2}** has been observed at all. The complex **3^{iPr_2}b** exhibits dynamic behavior which is frozen below −50 °C. Because the other complexes **3^{iPr_2}a**,**c**,**d** are not fluxional, the dynamic behavior should result from stereochemical nonrigidity of the ester moiety, i.e., interconversion between the s-trans and s-cis isomers, as shown in Scheme 2. Similar isomerization was noted for the Ru enolates obtained from cyanoacetate esters as reported by Murahashi.[3e]

Effect of the Substituents on the Tp^R Ligand: Dehydrative Condensation of Tp^{Me_2}Pd(py)−OH (1^{Me_2}) with Active Methylene Compounds 2 To Lead to Sequential Formation of N/O-Bound Enolato Complexes 3^{Me_2} and C-Bound Enolato Com-

(11) Ruiz, J.; Rodriguez, V.; López, G.; Casabó, J.; Molins, E.; Miravitlles, C. *Organometallics* **1999**, *18*, 1177.

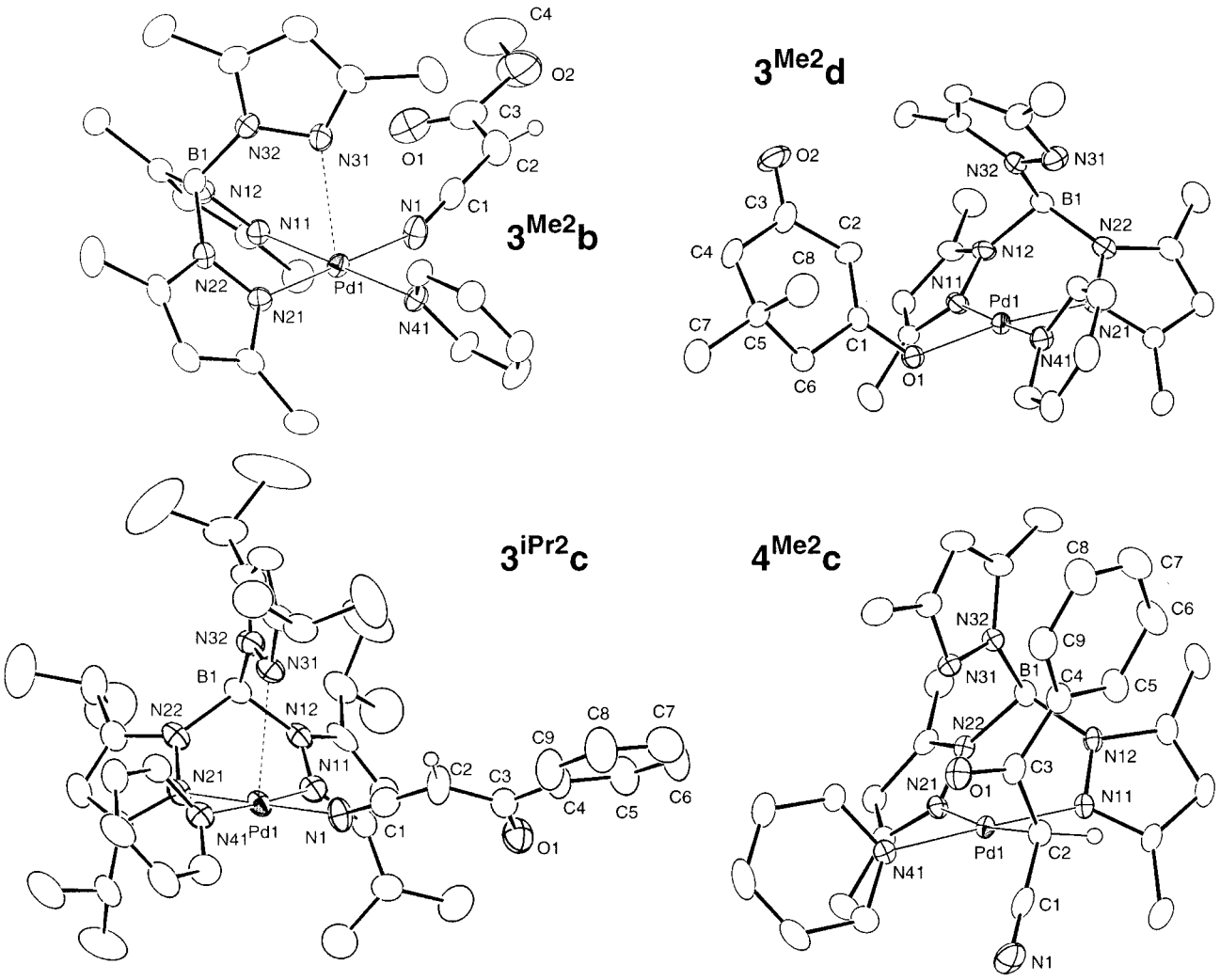

Figure 1. Molecular structures of the (enolato)palladium complexes $\mathbf{3}^{\mathbf{Me_2}}\mathbf{b}$, $\mathbf{3}^{\mathbf{iPr_2}}\mathbf{c}$, $\mathbf{3}^{\mathbf{Me_2}}\mathbf{d}$, and $\mathbf{4}^{\mathbf{Me_2}}\mathbf{c}$ drawn (with displacement ellipsoid amplitudes) at the 30% probability level.

Table 2. Structural Parameters for the Core Parts of the Tp^RPd Complexes 3, 4, and 6[a]

	complex, X					
	$\mathbf{3}^{\mathbf{iPr_2}}\mathbf{c}$, N1	$\mathbf{3}^{\mathbf{Me_2}}\mathbf{b}$, N1	$\mathbf{3}^{\mathbf{Me_2}}\mathbf{d}$, O1	$\mathbf{4}^{\mathbf{Me_2}}\mathbf{c}$, C2	$\mathbf{6}^{\mathbf{iPr_2}}\mathbf{a}$, N3	$\mathbf{6}^{\mathbf{iPr_2}}\mathbf{b}$, N2
Pd1−N11	2.019(7)	2.006(2)	2.004(4)	2.009(3)	2.017(3)	2.005(6)
Pd1−N21	1.987(8)	2.017(3)	2.007(5)	2.068(3)	2.012(4)	2.023(7)
Pd1−N31	2.717(7)	2.794(2)	3.388(6)	3.003(3)	3.484(4)	3.494(6)
Pd1−N41	2.051(7)	2.021(2)	2.021(5)	2.039(3)	2.038(3)	2.046(7)
Pd1−X	2.00(1)	2.016(3)	1.990(4)	2.102(4)	2.033(4)	2.015(7)
N11−Pd1−N21	85.7(3)	86.7(1)	88.1(2)	86.3(1)	85.5(1)	86.9(2)
N11−Pd1−N31	82.7(2)	86.46(7)				
N11−Pd1−N41	176.7(3)	178.1(1)	176.3(2)	177.6(1)	175.1(1)	176.8(3)
N11−Pd1-X	94.4(3)	93.1(1)	94.9(2)	89.9(1)	94.9(1)	91.5(3)
N21−Pd1−N31	89.2(3)	82.92(7)				
N21−Pd1−N41	91.3(3)	91.7(1)	93.6(2)	92.3(1)	90.4(1)	90.4(3)
N21−Pd1−X	179.6(3)	179.5(1)	172.6(2)	172.5(1)	179.5(2)	178.2(2)
N31−Pd1−N41	95.8(2)	92.31(8)				
N31−Pd1−X	90.4(3)	97.50(9)				
N41−Pd1−X	88.6(3)	88.5(1)	83.9(2)	91.6(1)	89.2(1)	91.2(3)

[a] Interatomic distances in Å and bond angles in deg.

plexes $\mathbf{4}^{\mathbf{Me_2}}$. To examine the effect of the substituents attached to the pyrazolyl (pz) rings in the Tp^R ligand, the Tp^{Me_2} derivative $\mathbf{1}^{\mathbf{Me_2}}$ was subjected to dehydrative condensation. The reaction proceeded in a manner similar to that for the Tp^{iPr_2} derivative $\mathbf{1}^{\mathbf{iPr_2}}$ described above, but two different types of products were obtained, depending on the reaction conditions (Scheme 3). The condensation carried out at 0 °C afforded the N/O-bound enolato complexes $\mathbf{3}^{\mathbf{Me_2}}\mathbf{a}-\mathbf{d}$, whereas the condensation at ambient temperature followed by recrystallization from warm solvents produced the C-bound enolato complexes $\mathbf{4}^{\mathbf{Me_2}}\mathbf{a}-\mathbf{c}$, which were not observed for the Tp^{iPr_2} system. In addition, when $CDCl_3$ solutions of isolated samples of $\mathbf{3}^{\mathbf{Me_2}}\mathbf{a}-\mathbf{c}$ were heated at 50 °C, isomerization occurred over a period of 2 h to give the C-bound enolate $\mathbf{4}^{\mathbf{Me_2}}\mathbf{a}-\mathbf{c}$. These observations reveal

Table 3. Selected Spectroscopic Data for 6

	IR/cm^{-1} [a]		^{1}H NMR/δ_H [b–d]		
compd	BH	others	4-pz-H	others	^{13}C NMR/δ_C [c–e]
6^{iPr_2}a	2498	3268,[i] 2258,[f] 2201,[f] 2177,[f] 1609[g]	5.72 5.91 6.01	2.51, 2.64 (2H, AB q, J = 16, CH_2), 5.72 (1H, br, NH)	47.9 (s, =*C*(CN)$_2$), 53.4 (t. J = 177, CH_2), 112.9 (t, J = 15, CH_2*C*N), 117.4, 118.3 (s × 2, =C(*C*N)$_2$), 170.3 (s, N−*C*=)
6^{iPr_2}b	2482	3221,[i] 2184,[f] 1743,[h] 1651,[h] 1609[g]	5.69 5.82 5.98	2.55, 2.72 (2H, AB q, J = 17, CH_2), 3.27, 3.65 (3H × 2, s × 2, OMe), 8.89 (1H, br, NH)	42.9 (t. J = 132, CH_2), 50.2, 51.3 (q × 2, J = 147 Hz, OMe), 68.4 (s, =*C*CN), 122.0 (s, CN), 168.3 (s, N−*C*=), 171.1, 173.3 (s × 2, *C*=O)
6^{Me_2}a	2485	3275,[i] 2257,[f] 2199,[f] 2173,[f] 1610[g]	5.70 5.84 5.95	2.89, 2.98 (2H, AB q, J = 16, CH_2), 5.76 (1H, br, NH)	23.9 (t, J = 137, CH_2), 47.7 (s, =*C*(CN)$_2$), 113.3 (t, J = 11, CH_2*C*N), 117.6, 118.5 (s × 2, =C(*C*N)$_2$), 170.3 (s, N−*C*=)

[a] Observed as KBr pellets. [b] Observed at 400 MHz in $CDCl_3$ at room temperature unless otherwise stated. [c] Multiplicities and coupling constants (in Hz) are shown in parentheses. Signals are singlets unless otherwise stated. [d] Other signals are reported in the Experimental Section. [e] Observed at 100 MHz in $CDCl_3$ at room temperature unless otherwise stated. [f] ν_{CN}. [g] ν_{py}. [h] ν_{CO}. [i] ν_{NH}.

Scheme 2

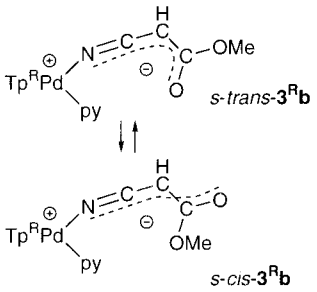

Scheme 3

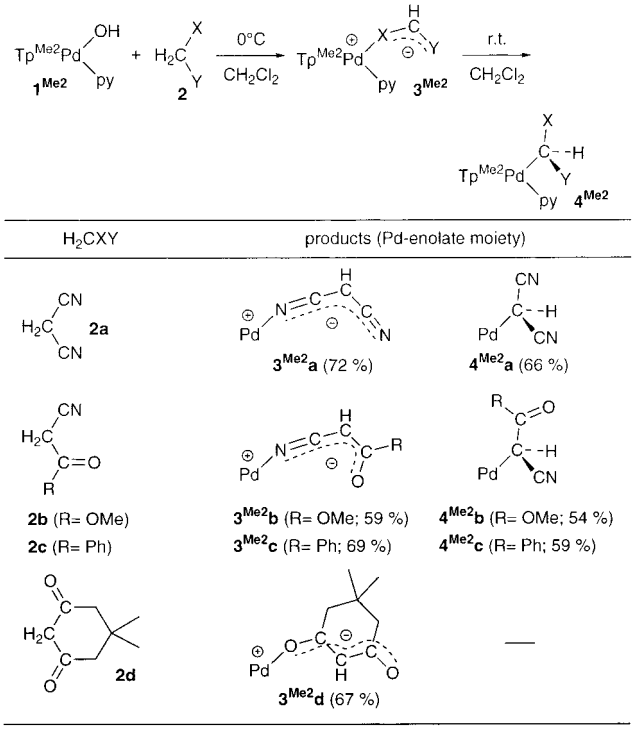

Scheme 4

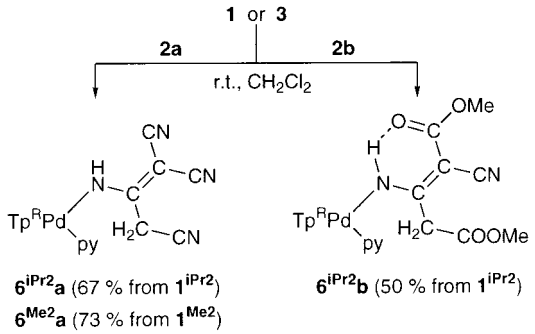

that, in the present Tp^{Me_2}Pd system, the N/O-bound enolates **3^{Me_2}** and C-bound enolates **4^{Me_2}** are the kinetic and thermodynamic products, respectively, of the dehydrative condensation of the hydroxo complexes **1^{Me_2}** with active methylene compounds **2**. However, no isomerization was observed for **3^{Me_2}d** obtained from dimedone **2d**, presumably due to the steric repulsion, because the C-bound form contains the highly congested secondary Pd−CHXY moiety.

The N/O-bound enolates **3^{Me_2}a**−**d** are readily characterized by comparison of their spectroscopic features with those of the Tp^{iPr_2} derivatives **3^{iPr_2}a**−**d** discussed above, and the molecular structures of **3^{Me_2}b**,**d** obtained from methyl cyanoacetate **2b** and dimedone **2d** have been determined by X-ray crystallography (Figure 1 and Table 2; for discussion, see below). In contrast to the Tp^{iPr_2} derivatives **3^{iPr_2}**, fluxional behavior was observed for **3^{Me_2}a**−**c**. Although the dynamic behavior of **3^{Me_2}b** can be interpreted in terms of the mechanism shown in Scheme 2, the mechanism for the other derivatives **3^{Me_2}a,c** should involve pseudorotation of the Tp^{Me_2} ligand, as already discussed for the related square-planar Tp^{R}Rh^I complexes.[6a,j,n,12] The mechanism for **3^{Me_2}b** at higher temperature may be associated with a similar pseudorotation of the Tp^{Me_2} ligand.

As for the C-bound enolates **4^{Me_2}**, the Pd−CH linkage can be confirmed by (1) the upfield shift of the methine carbon signals by 20−30 ppm compared to those of **3^{Me_2}**, (2) the change of the $^1J_{CH}$ value of the Pd−CH moiety to ∼150 Hz, consistent with sp^3 hybridization, and (3) the upfield shift of the δ_C(CN) signals to the normal uncoordinated CN region (∼120 ppm)). The molecular structure of **4^{Me_2}c** has been verified by X-ray crystallography (Figure 1 and Table 2; for a detailed discussion, see below).

Dimerization of Cyano Compounds by 1 to Give 2-Cyanoethenylamido Complexes 6. The condensation of **1** in the presence of an excess amount of dicyanomethane (**2a**) and methyl cyanoacetate (**2b**) afforded the (2-cyanoethenyl)amido complexes **6a**,**b** (Scheme 4), which showed the characteristic ν_{NH} absorption in addition to a couple of ν_{CN} and/or ν_{CO} vibrations (Table 3). The Tp^{iPr_2} derivatives **6^{iPr_2}a**,**b** were

(12) See references cited in 6a,j,n.

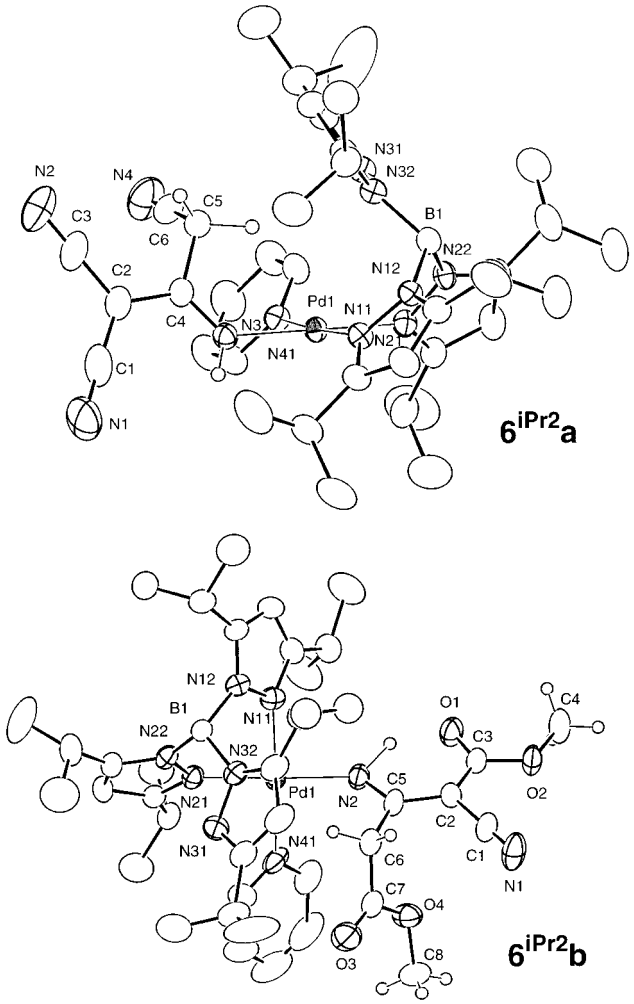

Figure 2. Molecular structures of the ((2-cyanoethenyl)-amido)palladium complexes $\mathbf{6^{iPr_2}a}$ and $\mathbf{6^{iPr_2}b}$ drawn (with displacement ellipsoid amplitudes) at the 30% probability level.

characterized by X-ray crystallography (Figure 2 and Table 2). However, reaction between $\mathbf{1^{Me_2}}$ and **2b** gave a mixture of products, and an analogous product was not formed from benzoylacetonitrile **2c**. The dimeric condensates **6a**,**b** were also obtained by treatment of the 1:1 condensates **3** with the corresponding cyano compounds, but no catalytic formation of the dimerized organic product ($YCH_2(H_2N)C{=}C(CN)(Y)$; Y = CN, COOMe) was observed even when **1** or **3** was heated in the presence of an excess amount of cyano compounds.

It is noteworthy that, of the two types of $Tp^{Me_2}Pd-$enolato complexes, i.e., the N- ($\mathbf{3^{Me_2}a}$) and C-bound species ($\mathbf{4^{Me_2}a}$), only the N-bound enolate $\mathbf{3^{Me_2}a}$ afforded the condensate $\mathbf{6^{Me_2}a}$ and no trace of the product was formed from the C-bound species $\mathbf{4^{Me_2}a}$ even under forced conditions. This result clearly indicates that the N-bound species **3** is the intermediate of the dimerization, giving **6**, and the C-bound species **4** is inactive for the dimerization.

The highly functionalized alkenyl moieties in **6** are characterized by spectroscopic as well as crystallographic analyses. The δ_C signals for the alkenyl carbon atoms, one with the two electron-withdrawing groups (CN and COOMe) and the other with the two electron-donating groups (NH and alkyl groups), are much separated (>100 ppm).[3c,10] The C=C bond is highly polarized, due to contribution of the zwitterionic forms **6A**,**A′** and **6B**, as is indicated by (1) the N−C lengths being shorter than the normal length (1.38 Å; values shown with **6** (Chart 1) are normal lengths (in Å) for each bond) by 0.07−0.08 Å and (2) the elongated C=C lengths. In the case of $\mathbf{6^{iPr_2}a}$ the negative charge is delocalized over the CN group cis to the NH group (**6A**), as suggested by the shorter C1−C2 bond (cf. C2−C3) and the longer C1−N1 bond (cf. C3−N2 and C6−N4). No significant delocalization over the ester moiety is evident for $\mathbf{6^{iPr_2}b}$, judging from the similar C2−C3 and C2−C1 lengths (**6A′**), although the ester oxygen atom (O1) is hydrogen-bonded with the N−H proton. The hydrogen bond causes elongation of the C3−O1 distance (cf. C7−O3). The presence of the amino groups is also indicated by the ν_{NH} vibrations and the δ_H(NH) signals, and the fact that the absorption for $\mathbf{6^{iPr_2}b}$ is weaker and lower in energy than that of $\mathbf{6^{iPr_2}a}$ should be a result of the intramolecular hydrogen bonding.

Reaction of the obtained enolato complexes **3** and **4** with electrophiles, including benzaldehyde, was also examined, but no reaction was observed.[13]

Discussion

Molecular Structures of Tp^RPd-Enolato Complexes 3 and 4. (i) Structures of the Enolato Moieties. Two N-bound complexes ($\mathbf{3^{Me_2}b}$ and $\mathbf{3^{iPr_2}c}$), one O-bound species ($\mathbf{3^{Me_2}d}$), and one C-bound enolato complex ($\mathbf{4^{Me_2}c}$) have been characterized by X-ray crystallography (Figure 1), and the structural parameters for the enolato parts are summarized in Chart 2 (The upper and lower values shown for N-bound enolates are for $\mathbf{3^{iPr_2}c}$ and $\mathbf{3^{Me_2}b}$, respectively.). Other parameters are listed in Table 2.

For the structure of the C-bound enolate $\mathbf{4^{Me_2}c}$, no significant electron delocalization is evident and all the bond lengths for $\mathbf{4^{Me_2}c}$ shown in Chart 2 are in good agreement with the values reported for typical bond lengths (Pd−C = 2.071 Å ($(Tp^{iPr_2})(PPh_3)Pd-Me$);[15] $C(sp^3)-C(sp)$ = 1.47 Å, $C(sp)\equiv N(sp)$ = 1.14 Å, $C(sp^3)-C(sp^2)$ = 1.51 Å, $C(sp^2)-C(sp^2)$ = 1.48 Å, $C(sp^2){=}O(sp^2)$ = 1.21 Å),[2c] and the structural parameters for the Pd−CH(CN) moiety are comparable to those of $[(C_6F_5)_4Pd_2[\mu\text{-}CH(CN)-CN]_2$ reported by López.[11] The slight elongation of the C1−C2 bond should be due to the contribution of an η^2-(C1=C2) form,[14] although the Pd1−C2−C1 angle is not acute, as would be anticipated for such an η^2 structure.

Complex $\mathbf{4^{Me_2}c}$ contains two chiral centers (Pd1 and C2), but only one diastereomer has been detected by spectroscopic and crystallographic analyses. The observed structure should be a result of minimizing steric repulsions in the molecule.

In contrast to the C-bound enolate $\mathbf{4^{Me_2}c}$ discussed above, significant deformation from the localized form **3A** is observed for the N-bound enolates ($\mathbf{3^{Me_2}b}$ and $\mathbf{3^{iPr_2}c}$), in particular, for the latter derived from ben-

(13) Komiya reported that the Re−enolate $[(PhMe_2P)_4\{R'OC(=O)-CHRCN\}Re]^+$ did not react with aldehyde but reacted in the presence of a proton donor, revealing the importance of proton.[4d] However, no condensation was observed under similar reaction conditions.

(14) So-called β-effect: Ariyaratne, J. K.; Bierrum, A. M.; Green, M. L. H.; Ishaq, M.; Prout, C. K.; Swanwick, M. G. *J. Chem. Soc. A* **1969**, 1309.

(15) Tanaka, M.; Akita, M. Unpublished results.

Chart 1

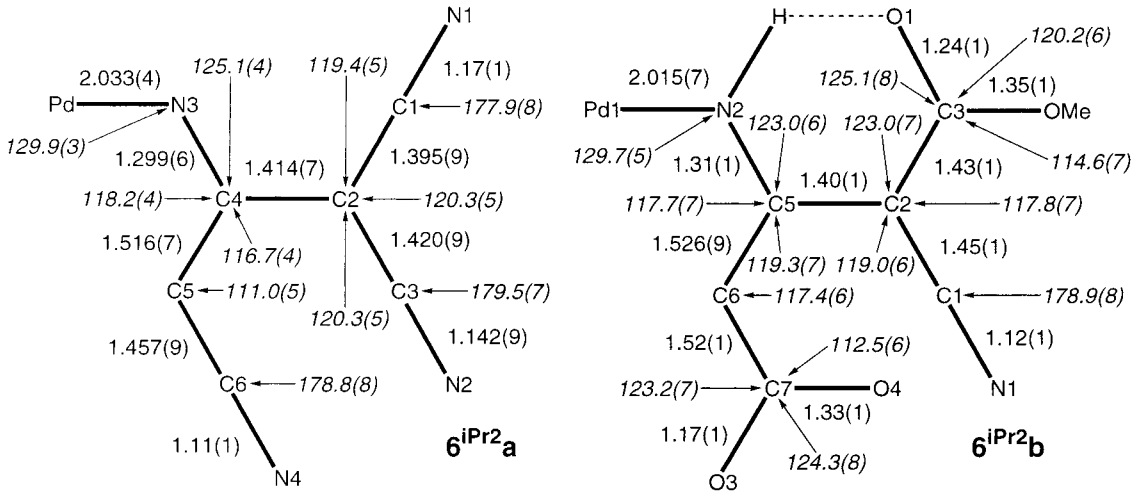

[roman: bond lengths (in Å); *italic*: bond angles (in deg)]

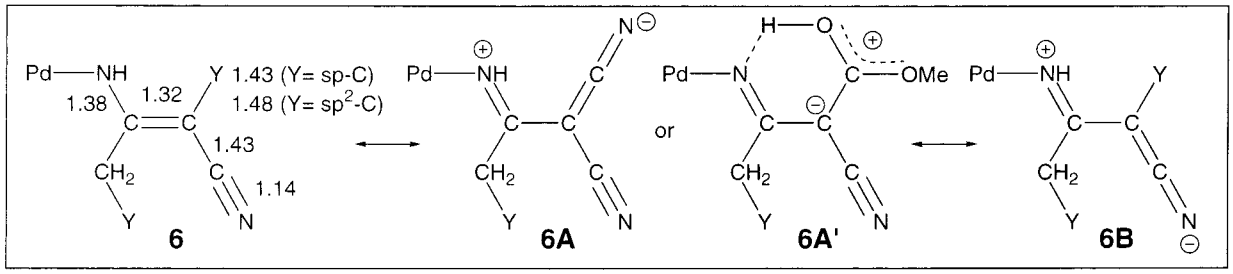

Chart 2

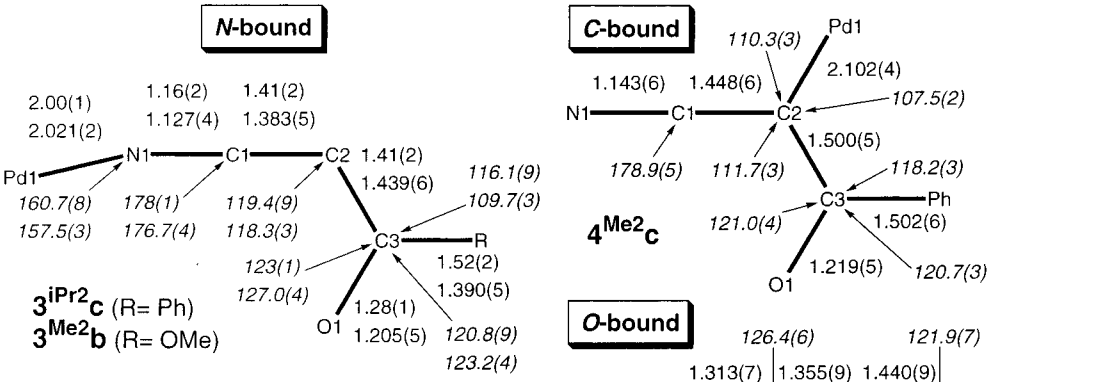

[roman: bond lengths (in Å); *italic*: bond angles (in deg)]

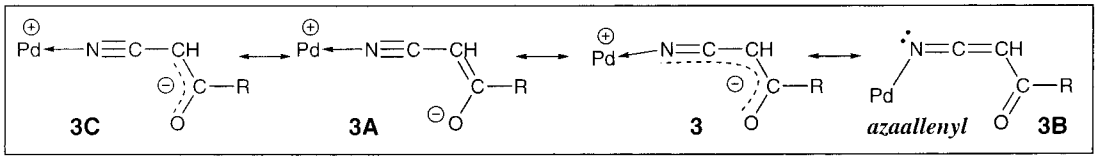

zoylacetonitrile **2c**. It is notable for $\mathbf{3}^{\mathbf{iPr_2}}\mathbf{c}$ that the C1−C2 and C2−C3 distances are substantially shorter than the corresponding bond lengths of the C-bound enolate $\mathbf{4}^{\mathbf{Me_2}}\mathbf{c}$, whereas the C3−O1 separation is longer than the corresponding C3−O1 distance of $\mathbf{4}^{\mathbf{Me_2}}\mathbf{c}$, indicating delocalization of the negative charge over the N1−C1−C2−C3−O1 linkage, as typically depicted for **3**. Although similar deformation is observed for the other N-bound enolate $\mathbf{3}^{\mathbf{Me_2}}\mathbf{b}$, the extent of the deformation is smaller than that of $\mathbf{3}^{\mathbf{iPr_2}}\mathbf{c}$. In addition, because the C3−O1 length is comparable to the localized C(sp^2)=O(sp^2) length (1.21 Å), the delocalization may not be effectively extended to the ester moiety, presumably due to π-donation from the methoxy group (R). In both of the N-bound enolates the Pd−N−C linkage is bent from a linear structure by ca. 10°. The bending could be

attributed to the contribution of the azaallenyl structure **3B**,[16] because no severe steric repulsion between the enolato ligand and the $Tp^RPd(py)$ backbone is found.

Similar structural features were already pointed out for the related Ru− and Re−enolato complexes derived from cyanoacetate esters, $L_nM-NCCHC(=O)OR$ (L_nM = $(Ph_3P)_3(H)\{ROC(=O)CH_2CN\}Ru$,[3b] $[(PhMe_2P)_4\{R'OC(=O)CHRCN\}Re]^+$,[4b,c] (dppe)(cod)(H)Ru,[4d] Cp(dppe)Ru).[3d] Although the authors proposed an oxo-π-allyl structure such as **3C**, the NC−C distances (1.30−1.40 Å), which are shorter than or comparable to the corresponding distances of our complexes, reveal the double-bond character for the NC−C moiety. We therefore conclude that structure **3**, in which the negative charge is delocalized over the N−C−C−Y linkage, can best describe the structural features of the N-bound enolates. The M−N−C angles of **3** being slightly more acute than those of the Ru and Re complexes (166−176°)[3,4] indicate the increased contribution of the azaallenyl structure **3B**.[16]

Averaging of the bond lengths of the enolato moiety is also observed for the O-bound enolate $\mathbf{3^{Me_2}d}$, but the C2−C3−O2 moiety is not as deformed as the Pd−O1−C1−C2 moiety is. Although these structural features suggest that delocalization of π-electrons may not be extended to the C3−O2 part, the ν_{CO} absorption appearing at 1611 cm^{-1} clearly indicates that the C3═O2 bond order is substantially decreased due to the delocalization.

Thus it has been revealed that, in the N/O-bound enolates **3** π-electrons are delocalized over the two functional groups (X and Y) attached to the central methine carbon atom, in contrast to the C-bound enolate **4**, where the structure can be described by the localized canonical form. Contribution of the azaallenyl form **3B** is also indicated by the bending of the Pd−N−C linkage.

(ii) Structure of the $Tp^RPd(py)$ Backbone. The Pd coordination planes (Pd1−N11−N21−N41−X; X = the coordinating atom of the enolato ligands) are essentially planar, judging from the interligand angles close to the right angle, the linear N11−Pd1−N41 and N21−Pd1−X linkages, and the sum of the interligand angles (360.0−360.5°).

The enolato complexes can be divided into two groups on the basis of the presence/absence of the coordination of the third pz groups (N31), i.e., the N31−Pd1 distance (Table 2). The Tp^R ligand in the N-bound enolates $\mathbf{3^{Me_2}b}$ and $\mathbf{3^{iPr_2}c}$, where the Pd1−N31 separations are ∼2.8 Å, are κ^3-coordinated to the Pd center. Although the Pd1−N31 distances are considerably longer than the other Pd1−N distances in the basal plane and the sum of atomic radii of Pd and N (∼2.1 Å), the orientation of the third pz ring indicates some bonding interaction between them. The lone pair electrons of N31 are projected toward the Pd center. In contrast to the N-bound enolates, the Pd1−N31 separation of the O-bound ($\mathbf{3^{Me_2}d}$) and C-bound enolates ($\mathbf{4^{Me_2}c}$) are longer than 3.0 Å, which exceeds the range for a bonding interaction.

The coordination behavior of the third pz ring can be interpreted in terms of a combination of Lewis acidity of the Pd center and the steric effects of the Tp^R and enolato ligands. In general, the Lewis acidity of the metal center increases as the ligand system becomes more electron withdrawing (electronegative). Therefore, the Pd center in an N-bound enolato complex coordinated by the more electronegative nitrogen atom should be more Lewis acidic than that in a C-bound enolato complex. As a result, the third pz ligand in the N-bound enolates would be coordinated to the more Lewis acidic Pd center to lead to a square-pyramidal structure with the κ^3-Tp^R ligand. Although the lone pair electrons of the third pz ring of the C-bound isomer $\mathbf{4^{Me_2}c}$ appear to be projected toward the Pd center, this should result from the $\pi-\pi$ stacking between the pz and Ph rings of the enolato moiety (distances between the two rings ranging from 3.455(5) (C4−C31) to 4.282(7) Å (C7−C33); dihedral angle between the rings 18.7(2)°), as can be seen from the molecular structure, and bonding interaction is negligible, judging from the Pd1−N31 separation (3.003(3) Å) (Figure 1). These considerations, however, are not consistent with the κ^2 coordination of the Tp^{Me} ligand in $\mathbf{3^{Me_2}d}$, bearing a more electron-withdrawing O-coordinated enolato ligand. This inconsistency could be attributed to the steric repulsion between the Tp^{Me} and enolato ligands. As can be seen from the molecular structures, the N-bound enolato ligand of the cyano derivatives with the linear N−C−C does not virtually suffer from steric repulsion with the other parts of the complex, whereas the O-enolate of dimedone, being much bulkier than the N-bound enolates, may prevent coordination of the third pz ring.

Scheme 5

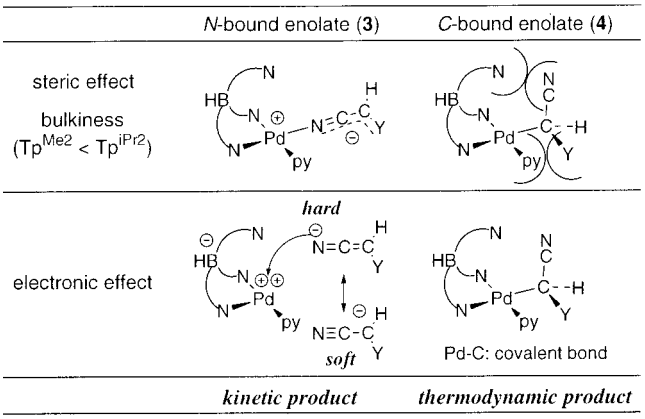

Factors Determining the Structures of the Tp^RPd−Enolato Complexes: N-Bound vs C-Bound. Comparison of the results for the $Tp^{iPr_2}Pd$ and $Tp^{Me_2}Pd$ systems reveals that dehydrative condensation between the hydroxopalladium complex **1** and active methylene compounds containing the cyano group **2** affords the N-bound enolates **3** as the kinetic products and the C-bound enolates **4** as the thermodynamic products. This result can be interpreted in terms of steric and electronic effects (Scheme 5).

The linear cyano−enolato ligand in N-bound enolates **3** suffers from steric repulsion with the Tp^R and py ligands to a much smaller extent than the secondary alkyl enolate group in C-bound species **4** does. A similar structural effect of the metal fragment has been already noted for the $Cp(R_3P)_2Ru-CH(CN)(SO_2Ph)$ system by Murahashi,[3d] where the distribution of N- and C-bound

(16) Badley, W. H.; Choudhury, P. *J. Organomet. Chem.* **1973**, *60*, C64. Suzuki, K.; Nakamura, S. *Inorg. Chim. Acta* **1977**, *25*, L21. Suzuki, K.; Sakurai, M. *Inorg. Chim. Acta* **1979**, *32*, L3.

Scheme 6

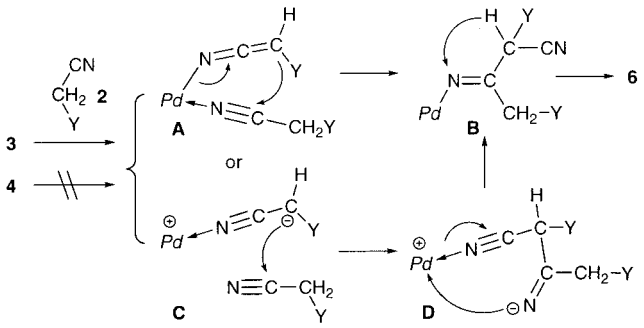

isomers is dependent on the bulkiness of the phosphine ligand (PR_3); i.e., a compact phosphine with a small cone angle leads to the C-bound enolate, whereas a bulky phosphine affords the N-bound enolate.

As for electronic effects, the enolato complexes should be formed by coupling between the enolate anion and the cationic $[Tp^RPd(py)]^+$ species generated by dehydration. Because the negative charge of the Tp^R anion is localized on the B atom, the Pd center is the virtually +2-charged, hard center. When the two canonical forms of the cyano−enolate, where the negative charge is localized on the N and C atoms, respectively, are taken into account, the hard Pd center should prefer coupling with the hard N-enolate to that with the soft C-enolate. The formation of the dinuclear μ-malononitrilate complex $[(C_6F_5)_4Pd_2[\mu\text{-}CH(CN)CN]_2]$ was interpreted in terms of dimerization of the initially generated mononuclear C-bound enolato complex $[(H_2O)(C_6F_5)Pd-CH(CN)_2]$.[11] The difference could be attributed to the soft hydrocarbyl groups (C_6F_5) making the palladium center soft.

In both aspects, formation of the N-bound enolate $\mathbf{3^{Me_2}}$ rather than the C-bound enolate $\mathbf{4^{Me_2}}$ seems to be the preferable reaction pathway, and therefore, the N-bound species $\mathbf{3^{Me_2}}$ should be formed as the kinetic product. The C-bound species $\mathbf{4^{Me_2}}$ containing the covalent Pd−C bond, however, may be more stable than the zwitterionic N-bound form $\mathbf{3^{Me_2}}$. In the case of Tp^{iPr_2} complexes, the bulky Tp^{iPr_2} ligand prohibits conversion into the C-bound form, and the N-bound form $\mathbf{3^{iPr_2}}$ is the kinetic as well as thermodynamic product.

Dimerization of Cyano Compounds. Reaction of the hydroxo complex **1** with an excess amount of cyano compounds **2a**,**b** or reaction of the 1:1 condensate **3** with **2a**,**b** resulted in stoichiometric dimerization of the cyano compound **2** to produce the 1:2 condensate, i.e., the 2-cyanoethenylamido complex **6**, in a specific manner.[17] The most important reaction aspect is that the C-bound enolate $\mathbf{4^{Me_2}}$ did not react with **2** any more and remained unreacted.

On the basis of the results obtained, possible reaction mechanisms are shown in Scheme 6. Coordination of the cyano compound to the Pd center would form the five-coordinate intermediate **A**, and the subsequent electrocyclic reaction should afford the imino intermediate **B**, which is finally converted to the 1:2 condensate **6** via a H-shift. Another possible mechanism involves nucleophilic attack of the carbanion at the cyano carbon atom of the external cyano compound **C** followed by replacement of the coordinated cyano group by the resultingimide anion (**D**). Because the obtained enolato complexes **3** and **4** are not reactive enough to be coupled with other electrophiles as mentioned above, the former mechanism seems to be preferable to the latter one. The low reactivity of the enolato complexes may be ascribed to the small electron density at the enolate carbon atom due to (1) delocalization of the anionic charge over the enolate linkage and (2) the electrostatic attractive interaction between the negative charge on the enolato moiety and the virtually +2-charged Pd center (see above). In addition, because the Pd−N bond in **6** is not basic enough to be protonated by $NC-CH_2-Y$ (**2**), catalytic production of the dimeric organic product $YCH_2(H_2N)C{=}C(CN)(Y)$ is not observed. Dimerization of active methylene compounds containing a cyano group has been successfully catalyzed by a hydridoiridium complex as reported by Murahashi, who originally proposed a C-bound enolate as the reaction intermediate[3c] but, in their recent account, reported that an N-bound enolato species was active for the dimerization.[3g]

Conclusions. The present study reveals the following aspects of the enolatopalladium complexes bearing the Tp^R and py ancillary ligands, as summarized in Scheme 7.

Scheme 7

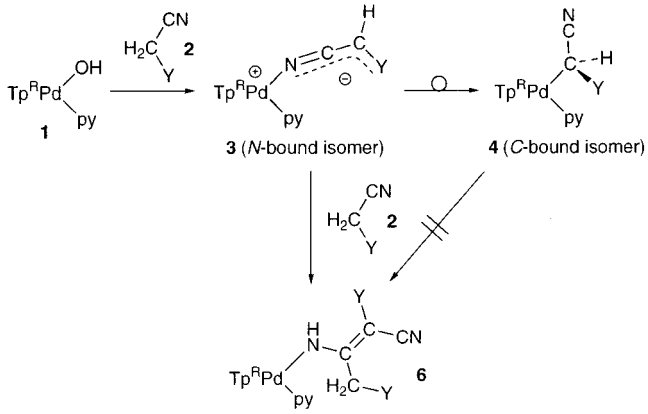

(1) The enolato complexes $(Tp^R)(py)Pd$-enolato (**3** and **4**) are obtained by dehydrative condensation between the hydroxopalladium complex $(Tp^R)(py)Pd-OH$ (**1**) and active methylene compounds $CH_2(X)(Y)$ (**2**).

(2) Of the two possible isomeric N- ($\mathbf{3^{Me_2}}$) and C-bound $(Tp^{Me_2})(py)Pd$−enolato complexes ($\mathbf{4^{Me_2}}$) derived from cyano compounds, the former is the kinetic product and the latter is the thermodynamic product and the former complex is gradually converted to the latter isomer. However, enolato complexes with the bulky Tp^{iPr_2} ligand forms only the N-bound isomer $\mathbf{3^{iPr_2}}$, due to steric repulsion between the Tp^{iPr_2} ligand and the C-bound, secondary alkyl moiety.

(3) Both the N/O- and C-bound enolates are characterized by a combination of spectroscopic and crystallographic analyses, and the two isomers are readily discriminated on the basis of the ν_{CN}, $\delta_C(CH)$, and $^1J_{CH}(CH)$ values.

(4) The 2-cyanoethenylamido complex **6** is obtained by reaction between the hydroxo complex **1** and cyano

(17) Attempted cross-condensation ($\mathbf{3^{iPr_2}a}$ + **2b** or MeCN; $\mathbf{3^{iPr_2}b}$ + **2a** or MeCN) resulted in the formation of a mixture of products. Formation of condensates was suggested by the appearance of the ν_{NH} vibrations of the Pd−NH moiety.

compounds **2a**,**b**. The 1:2 condensate **6** is also obtained from the N-bound isomer **3** but not from the C-bound isomer **4**.

Experimental Section

General Methods. All manipulations were carried out under an Ar atmosphere using standard Schlenk tube techniques. Hexane and CH_2Cl_2 were dried over Na−K/benzophenone and CaH_2, respectively, under Ar and distilled just before use. NMR spectra were recorded on a JEOL EX-400 spectrometer (^{1}H, 400 MHz; ^{13}C, 100 MHz). $CDCl_3$ and CD_2Cl_2 for NMR measurements containing 0.5% TMS were dried over molecular sieves and distilled under reduced pressure. IR spectra (KBr pellets) were obtained on a JASCO FT/IR 5300 spectrometer. The hydroxo complexes $\mathbf{1}^{\mathbf{iPr_2}}$ and $\mathbf{1}^{\mathbf{Me_2}}$ were prepared by hydrolysis of the corresponding chloride complexes (Tp^R)(py)Pd−Cl with aqueous NaOH solution.[7a]

Preparation of $\mathbf{3}^{\mathbf{iPr_2}}$. As a typical example, the preparative procedure for $\mathbf{3}^{\mathbf{iPr_2}}\mathbf{a}$ is described and $\mathbf{3}^{\mathbf{iPr_2}}\mathbf{b,c}$ were prepared in a manner similar to the synthesis of $\mathbf{3}^{\mathbf{iPr_2}}\mathbf{a}$. To $\mathbf{1}^{\mathbf{iPr_2}}$ (264 mg, 0.395 mmol) dissolved in CH_2Cl_2 (5 mL) was added Na_2SO_4 (ca. 150 mg). A CH_2Cl_2 solution (15 mL) of $CH_2(CN)_2$ (26 mg, 0.394 mmol) was added dropwise to the mixture at ambient temperature. The resultant mixture was stirred for 1 h and filtered through a Celite pad to remove solids. The filtrate was concentrated under reduced pressure, and crystallization from CH_2Cl_2−hexane gave $\mathbf{3}^{\mathbf{iPr_2}}\mathbf{a}$ as a yellow solid (156 mg, 0.218 mmol, 55% yield). ^{1}H NMR ($CDCl_3$; at room temperature): δ_H 8.61 (2H, d, 6 Hz, *o*-py), 7.83 (1H, t, J = 8 Hz, *p*-py), 7.35 (2H, t, J = 7 Hz, *m*-py), 3.50 (1H, sept, J = 7 Hz, C*H*Me$_2$), 3.43 (2H, sept, J = 7 Hz, C*H*Me$_2$), 2.92, 2.69, 2.05 (1H × 3, sept × 3, J = 7 Hz, C*H*Me$_2$), 0.55−1.42 (36H, m, CH*Me*$_2$). ^{13}C NMR ($CDCl_3$; at room temperature): δ_C 160.8, 159.3, 158.8, 157.8 155.3 (s × 5, 3,5-pz), 153.1 (d, J = 186 Hz, *o*-py), 139.0 (d, J = 165 Hz, *p*-py), 125.2 (d, J = 165 Hz, *m*-py), 99.2, 98.8, 98.1 (d × 3, J = 173 Hz, 4-pz), 28.6−20.2 (CH*Me*$_2$). Anal. Calcd for $C_{35}H_{52}BN_9Pd$: C, 58.71; H, 7.32; N, 17.60. Found: C, 58.51; H, 7.22; N, 17.56. Complexes $\mathbf{3}^{\mathbf{iPr_2}}\mathbf{b}$−$\mathbf{d}$ and $\mathbf{5}^{\mathbf{iPr_2}}\mathbf{e}$ were prepared in a manner similar to the synthesis of $\mathbf{3}^{\mathbf{iPr_2}}\mathbf{a}$. $\mathbf{3}^{\mathbf{iPr_2}}\mathbf{b}$ was obtained in 64% yield as yellow crystals. ^{1}H NMR (CD_2Cl_2; at −50 °C; an isomeric mixture): δ_H 8.48 (2H, d, J = 6 Hz, *o*-py), 7.81 (1H, t, J = 7 Hz, *p*-py), 7.31 (2H, t, J = 7 Hz, *m*-py), 3.6−2.0 (6H, m, C*H*Me$_2$), 1.36−0.38 (36H, m, CH*Me*$_2$). ^{13}C NMR (CD_2Cl_2; at −50 °C; an isomeric mixture): δ_C 160.5, 159.2, 158.9, 158.8, 157.7, 157.5, 157.3, 155.1 (s × 7, 3,5-pz), 152.9, 152.8 (d, J = 191 Hz, *o*-py), 140.5, 139.9 (s × 2, 3,5-pz), 139.3, 139.1 (d × 2, J = 166 Hz, *p*-py), 125.3, 125.1 (d × 2, J = 164 Hz, *m*-py), 99.2, 99.1, 99.0. 97.6 (d, J = 169 Hz, 4-pz), 20.8−27.9 (CHMe$_2$). Anal. Calcd for $C_{36}H_{55}BN_8Pd$: C, 57.72; H, 7.40; N, 14.96. Found: C, 57.99; H, 7.62; N, 14.72. $\mathbf{3}^{\mathbf{iPr_2}}\mathbf{c}$ was obtained in 68% yield as yellow crystals. ^{1}H NMR ($CDCl_3$; at room temperature): δ_H 8.81 (2H, d, J = 6 Hz, *o*-py), 7.78 (1H, t, J = 8 Hz, *p*-py), 7.74 (2H, dd, J = 6 and 3 Hz, *m*-Ph), 7.39 (2H, t, J = 7 Hz, *m*-py), 7.30 (2H, d, J = 2 Hz, *o*-Ph), 7.29 (1H, m, *p*-Ph), 3.66, 3.50, 3.48, 2.87 2.69, 2.11 (1H × 6, sept × 6, J = 7 Hz, C*H*Me$_2$), 1.38−0.59 (36H, m, CH*Me*$_2$). ^{13}C NMR ($CDCl_3$; at room temperature): δ_C 161.4, 159.3, 158.8, 158.0, 157.9, 155.3 (s × 6, 3,5-pz), 153.6 (d, J = 191 Hz, o-py), 141.7 (s, *ipso*-Ph), 138.9 (dt, J = 162 and 7 Hz, *p*-py), 136.2 (s, CN), 129.2 (dt, J = 162 and 7 Hz, *p*-Ph), 127.6 (dd, J = 161 and 4 Hz, *o*-Ph), 126.3 (dt, J = 158 and 5 Hz, *m*-Ph), 125.2 (dt, J = 167 and 6 Hz, *m*-py), 99.1, 98.9, 98.2 (d × 3, J = 173 Hz, 4-pz). Anal. Calcd for $C_{41}H_{57}BN_8OPd$: C, 61.93; H, 7.23; N, 14.09. Found: C, 62.25; H, 7.96; N, 13.77. $\mathbf{3}^{\mathbf{iPr_2}}\mathbf{d}$ was obtained in 66% yield as yellow crystals. ^{1}H NMR ($CDCl_3$; at room temperature): δ_H 8.84 (2H, d, J = 6 Hz, *o*-py), 7.76 (1H, t, J = 8 Hz, *p*-py), 7.29 (2H, t, J = 7 Hz, *m*-py), 3.58 (2H, m, C*H*Me$_2$), 3.33, 3.00, 2.68, 2.09 (1H × 4, sept × 6, J = 7 Hz, C*H*Me$_2$), 1.40−0.87 (36H, m, CH*Me*$_2$). ^{13}C NMR ($CDCl_3$; at room temperature): δ_C 161.5, 159.1, 157.8, 157.4, 154.7 (s × 5, 3,5-pz), 152.4 (dd, J = 187 and 4 Hz, *o*-py), 138.4 (dt, J = 165 and 6 Hz, *p*-py), 124.4 (dt, J = 167 and 6 Hz, *m*-py), 99.1, 99.0, 98.7 (d × 3, J = 173 Hz, 4-pz), 28.5−20.8 (CHMe$_2$). Anal. Calcd for $C_{40}H_{62}BN_7O_2Pd$: C, 60.80; H, 7.91; N, 12.41. Found: C, 60.68; H, 7.95; N, 12.00. $\mathbf{5}^{\mathbf{iPr_2}}\mathbf{e}$ was obtained in 64% yield as yellow crystals. ^{1}H NMR ($CDCl_3$; at room temperature): δ_H 3.5 (6H, br, C*H*Me$_2$), 1.5−1.0 (36H, m, CH*Me*$_2$). ^{13}C NMR ($CDCl_3$; at room temperature): δ_C 157.0, 159.9 (s × 2, 3,5-pz), 98.1 (d, J = 171 Hz, 4-pz), 27.7 − 22.9 (CHMe$_2$). Anal. Calcd for $C_{32}H_{53}BN_6O_3Pd$: C, 55.94; H, 7.78; N, 12.23. Found: C, 55.60; H, 7.64; N, 12.56.

Preparation of $\mathbf{3}^{\mathbf{Me_2}}$. As a typical example the preparative procedure for $\mathbf{3}^{\mathbf{Me_2}}\mathbf{a}$ is described, and $\mathbf{3}^{\mathbf{Me_2}}\mathbf{b,c}$ were prepared in a manner similar to the synthesis of $\mathbf{3}^{\mathbf{Me_2}}\mathbf{a}$. To a CH_2Cl_2 solution (15 mL) of $\mathbf{1}^{\mathbf{Me_2}}$ (139 mg, 0.278 mmol) cooled to 0 °C was added Na_2SO_4 (ca. 150 mg) and $CH_2(CN)_2$ (18 mg, 0.272 mmol), and the resultant mixture was stirred for 1 h at the same temperature. Then the mixture was filtered through a Celite pad, the filtrate was concentrated, and crystallization from CH_2Cl_2−hexane at −20 °C gave $\mathbf{3}^{\mathbf{Me_2}}\mathbf{a}$ (110 mg, 0.207 mmol, 72% yield) as yellow crystals. ^{1}H NMR (CD_2Cl_2; at −50 °C): δ_H 8.57 (2H, d, J = 5 Hz, *o*-py), 7.85 (1H, t, J = 7 Hz, *p*-py), 7.36 (2H, t, J = 7 Hz, *m*-py), 2.35, 2.33, 2.30, 2.09, 2.06, 1.41 (3H × 6, s × 6, J = 7 Hz, Me). ^{13}C NMR (CD_2Cl_2; at −50 °C): δ_C 152.4 (d, J = 186 Hz, *o*-py), 150.3, 148.9, 148.2, 146.9, 146.5, 144.1 (s × 6, 3,5-pz), 139.4 (dt, J = 173 and 6 Hz, *p*-py), 125.6 (d, J = 169 Hz, *m*-py), 106.9, 106.5, 105.4 (d × 3, J = 170 Hz, 4-pz), 14.3, 13.3, 13.25, 13.16, 13.09, 11.9 (q × 6, J = 129 Hz, Me). Anal. Calcd for $C_{23.2}H_{28.4}BN_9Cl_{0.4}Pd$ ($\mathbf{3}^{\mathbf{Me_2}}\mathbf{a}\cdot 0.2CH_2Cl_2$): C, 49.34; H, 5.07; N, 22.32. Found: C, 49.32; H, 5.13; N, 22.31. $\mathbf{3}^{\mathbf{Me_2}}\mathbf{b}$ was obtained in 59% yield as yellow crystals. ^{1}H NMR (CD_2Cl_2; at −50 °C; an isomeric mixture): δ_H 8.60 (2H, d, J = 5 Hz, *o*-py), 7.83 (1H, t, J = 7 Hz, *p*-py), 7.33 (2H, t, J = 7 Hz, *m*-py), 1.4−2.9 (18H, m, Me). ^{13}C NMR (CD_2Cl_2; at −50 °C; an isomeric mixture): δ_C 157.1 (d, J = 190 Hz, *o*-py), 155.1, 153.4, 152.8, 151.4, 150.9, 148.6 (s × 6, 3,5-pz), 143.8, 143.7 (d × 2, J = 160 Hz, *p*-py), 130.0, 129.9 (d, J = 170 Hz, *m*-py), 111.3, 111.0, 109.9 (d × 3, J = 167 Hz, 4-pz), 18.9, 18.7, 17.8, 17.7, 17.6, 16.4, 16.3 (q × 6, J = 129 Hz, Me). Anal. Calcd for $C_{24}H_{31}BN_8O_2Pd$: C, 49.63; H, 5.38; N, 19.29. Found: C, 49.38; H, 5.49; N, 19.35. $\mathbf{3}^{\mathbf{Me_2}}\mathbf{c}$ was obtained in 69% yield as yellow crystals. ^{1}H NMR (CD_2Cl_2; at −80 °C): δ_H 8.74 (2H, br, *o*-py), 7.86 (1H, t, J = 7 Hz, *p*-py), 7.60 (2H, d, J = 7 Hz, *o*-Ph), 7.40 (2H, br, *m*-py), 7.26 (3H, m, *m*,*p*-Ph), 2.50, 2.31, 2.28, 2.20, 2.03, 1.41 (3H × 6, s × 6, Me). ^{13}C NMR (CD_2Cl_2; at −80 °C): δ_C 152.6 (d, J = 185 Hz, *o*-py), 150.5, 148.8, 148.4, 147.0, 146.3, 144.1 (s × 6, 3,5-pz), 139.4 (dt, J = 173 and 6 Hz, *p*-py), 125.7 (d, J = 169 Hz, *m*-py), 106.8, 106.5, 105.0 (d × 3, J = 170 Hz, 4-pz), 14.6, 13.3, 12.1 (q × 3, J = 125 Hz, Me). Anal. Calcd for $C_{29}H_{33}BN_8OPd$: C, 55.56; H, 5.31; N, 17.78. Found: C, 55.20; H, 5.60; N, 17.90. $\mathbf{3}^{\mathbf{Me_2}}\mathbf{d}$ was obtained in 67% yield as yellow crystals. ^{1}H NMR ($CDCl_3$; at room temperature): δ_H 8.91 (2H, d, J = 5 Hz, *o*-py), 7.82 (1H, t, J = 8 Hz, *p*-py), 7.34 (2H, t, J = 7 Hz, *m*-py), 2.56 (3H, s, Me), 2.44 (6H, s, Me × 2), 2.21, 2.11, 1.87 (3H × 3, s × 3, Me). ^{13}C NMR ($CDCl_3$; at room temperature): δ_C 152.2 (d, J = 186 Hz, *o*-py), 150.8 (s, 3,5-pz), 148.6, 147.6 (br × 2, 3,5-pz), 146.4 (s, 3,5-pz), 143.5, (br, 3,5-pz), 138.6 (dt, J = 165 and 6 Hz, *p*-py), 124.6 (dt, J = 167 and 7 Hz, *m*-py), 107.2, 106.9, 103.8 (d × 3, J = 170 Hz, 4-pz), 28.3, 28.1 (q × 3, J = 125 Hz, Me). Anal. Calcd for $C_{28}H_{38}BN_7O_2Pd$: C, 54.08; H, 6.16; N, 15.77. Found: C, 54.17; H, 6.15; N, 15.65.

Preparation of $\mathbf{4}^{\mathbf{Me_2}}$. As a typical example, the preparative procedure for $\mathbf{4}^{\mathbf{Me_2}}\mathbf{a}$ is described and $\mathbf{4}^{\mathbf{Me_2}}\mathbf{b,c}$ were prepared in a manner similar to the synthesis of $\mathbf{4}^{\mathbf{Me_2}}\mathbf{a}$. To a CH_2Cl_2 solution (20 mL) of $\mathbf{1}^{\mathbf{Me_2}}$ (162 mg, 0.324 mmol) was added Na_2SO_4 (ca. 150 mg) and $CH_2(CN)_2$ (21 mg, 0.318 mmol), and the resultant mixture was stirred for 1 h at room temperature. Then the mixture was filtered through a Celite pad, the filtrate was concentrated, and crystallization from CH_2Cl_2−hexane at −20 °C gave $\mathbf{4}^{\mathbf{Me_2}}\mathbf{a}$ (111 mg, 0.214 mmol, 66% yield) as yellow

Table 4. Crystallographic Data

	$3^{iPr_2}c\cdot 1.74CH_2Cl_2$	$3^{Me_2}b$	$3^{Me_2}d$	$4^{Me_2}c$	$6^{iPr_2}a\cdot CH_2Cl_2$	$6^{iPr_2}b\cdot 0.5CH_2Cl_2$
formula	$C_{42.74}H_{62.48}BN_6Cl_{3.48}Pd$	$C_{24}H_{31}BN_8O_2Pd$	$C_{28}H_{38}BN_7O_2Pd$	$C_{29}H_{33}BN_8OPd$	$C_{39}H_{56}BN_{11}Cl_2Pd$	$C_{40.5}H_{62}BN_9O_4ClPd$
fw	960.96	580.77	621.86	626.74	867.06	891.66
cryst syst	monoclinic	monoclinic	orthorhombic	monoclinic	monoclinic	triclinic
space group	$P2_1/n$	$P2_1/c$	$Pbca$	$P2_1/n$	$P2_1/n$	$P\bar{1}$
a/Å	13.606(2)	13.0558(6)	17.855(2)	8.6448(3)	16.5082(7)	10.378(3)
b/Å	16.630(1)	14.3339(8)	19.375(4)	17.7105(9)	14.0485(6)	22.092(4)
c/Å	23.331(2)	14.8052(8)	17.092(4)	18.9942(9)	21.2050(10)	10.381(3)
α/deg						98.43(2)
β/deg	102.653(2)	95.855(2)		92.759(3)	111.660(2)	97.843(4)
γ/deg						80.52(2)
V/Å^3	5150.8(8)	2756.1(2)	5912(1)	2904.7(2)	4570.5(4)	2306(1)
Z	4	4	8	4	4	2
d_{calcd}/g cm^{-3}	1.24	1.40	1.40	1.43	1.26	1.28
μ/cm^{-1}	5.81	7.09	6.65	6.77	5.62	5.08
2θ/deg	<55	<55	<55	<55	<55	<55
transmissn factor	0.41−0.94	0.73−0.93	0.38−0.94	0.74−0.93	0.61−0.95	0.57−0.95
no. of data collected	26 179	21 378	31 131	19 940	31 919	12 003
no. of unique data collected	10 788	6493	6411	6038	10345	8142
no. of unique data with $F > 4\sigma(F)$	5617	5843	4084	4620	7221	5121
no. of params refined	544	336	360	367	496	515
R1[a] for data with $F > 4\sigma(F)$	0.097	0.056	0.066	0.042	0.062	0.084
wR2[b] for all data	0.285	0.147	0.206	0.126	0.174	0.221

[a] $R1 = [\sum||F_o| - |F_c||]/\sum|F_o|$ (for data with $I > 4\sigma(F)$). [b] $wR2 = [\sum\{w(F_o^2 - F_c^2)\}^2/\sum\{w(F_o^2)^2\}]^{0.5}$; $w = 1/[\sigma^2(F_o^2) + (0.1000P)^2]$, where $P = [2F_c^2 + \mathrm{Max}(F_o^2,0)]/3$ (for all data).

crystals. ^{1}H NMR ($CDCl_3$; at room temperature): δ_H 9.23 (2H, d, J = 5 Hz, *o*-py), 7.86 (1H, t, J = 8 Hz, *p*-py), 7.44 (2H, t, J = 7 Hz, *m*-py), 2.45, 2.42, 2.36, 2.30, 2.08, 1.47 (3H × 6, s × 6, Me). ^{13}C NMR ($CDCl_3$; at room temperature): δ_C 152.7 (d, J = 185 Hz, *o*-py), 150.1, 148.8, 148.4, 147.3, 146.2, 143.3 (s × 6, 3,5-pz), 138.8 (dt, J = 167 and 6 Hz, *p*-py), 125.6 (dt, J = 169 and 6 Hz, *m*-py), 107.6, 106.6, 106.3 (d, J = 173 Hz, 4-pz), 14.1, 13.8, 13.6, 13.3, 12.6 (q × 5, J = 127 Hz, Me). Anal. Calcd. for $C_{23.1}H_{28.2}BN_9Cl_{0.2}Pd$: C, 49.88; H, 5.11; N, 22.66. Found: C, 49.80; H, 5.19; N, 22.53. **4^{Me_2}b** was obtained in 54% yield as yellow crystals. ^{1}H NMR ($CDCl_3$; at room temperature): δ_H 9.25 (2H, d, J = 5 Hz, *o*-py), 7.79 (1H, t, J = 4 Hz, *p*-py), 7.35 (2H, t, J = 7 Hz, *m*-py), 2.47, 2.44, 2.32, 2.26, 1.97, 1.47 (3H × 6, s × 6, Me). ^{13}C NMR ($CDCl_3$; at room temperature): δ_C 152.9 (d, J = 185 Hz, *o*-py), 150.3, 148.2, 147.4, 147.3, 145.9, 144.2 (s × 6, 3,5-pz), 138.2 (dt, J = 163 and 6 Hz, *p*-py), 124.8 (dt, J = 165 and 5 Hz, *m*-py), 107.7, 106.6, 106.2 (d × 3, J = 170 Hz, 4-pz), 14.8, 14.1, 13.8, 13.2, 13.1, 12.3 (q × 6, J = 125 Hz, Me). Anal. Calcd for $C_{24}H_{31}BN_8O_2Pd$: C, 49.63; H, 5.38; N, 19.29. Found: C, 49.36; H, 5.59; N, 19.25. **4^{Me_2}c** (59% yield; yellow crystals): ^{1}H NMR ($CDCl_3$; at room temperature): δ_H 9.70 (2H, d, J = 8 Hz, *o*-py), 7.83 (1H, t, J = 8 Hz, *p*-py), 7.38 (2H, t, J = 6 Hz, *m*-py), 7.26 (1H, t, J = 7 Hz, *p*-Ph), 7.07, (2H, d, J = 8 Hz, *o*-Ph), 6.97 (2H, t, J = 8 Hz, *m*-Ph), 2.63, 2.54, 2.32, 2.22, 1.55, 1.45 (3H × 6, s × 6, J = 7 Hz, Me). ^{13}C NMR ($CDCl_3$; at room temperature): δ_C 153.3 (d, J = 191 Hz, *o*-py), 150.3, 148.3, 147.7, 145.5, 142.6 (s × 5, 3,5-pz), 138.2 (dt, J = 165 and 6 Hz, *p*-py), 137.0 (s, 3,5-pz), 131.4 (dt, J = 165 and 7 Hz, Ph), 127.45, 127.49 (d × 2, J = 160 Hz, Ph), 124.5 (d, J = 167 Hz, *m*-py), 107.9, 106.1, 105.6 (d × 3, J = 170 Hz, 4-pz), 15.1, 13.9, 13.3, 13.1, 12.9 (q × 5, J = 125 Hz, Me). Anal. Calcd for $C_{29}H_{33}BN_8OPd$: C, 55.56; H, 5.31; N, 17.78. Found: C, 55.20; H, 5.66; N, 17.79.

Preparation of 6. As a typical example the preparative procedure for **6^{iPr_2}a** is described and **6^{iPr_2}b** and **6^{Me_2}a** were prepared in a manner similar to the synthesis of **6^{iPr_2}a**. To a CH_2Cl_2 solution (15 mL) of **1^{iPr_2}** (97 mg, 0.145 mmol) was added Na_2SO_4 (ca. 150 mg) and $CH_2(CN)_2$ (20 mg, 0.30 mmol), and the resultant mixture was stirred for 1 h at room temperature. Then the mixture was filtered through a Celite pad, the filtrate was concentrated, and crystallization from CH_2Cl_2−hexane at −20 °C gave **6^{iPr_2}a** (76 mg, 0.097 mmol, 67% yield) as yellow crystals. ^{1}H NMR ($CDCl_3$; at room temperature): δ_H 9.03 (2H, d, J = 5 Hz, *o*-py), 7.90 (1H, t, J = 8 Hz, *p*-py), 7.45 (2H, t, J = 7 Hz, *m*-py), 3.58, 3.27, 3.20, 3.12, 2.77, 1.83 (1H × 6, sept × 6, J = 7 Hz, C*H*Me$_2$), 1.42−0.61 (36H, m CH*Me$_2$*). ^{13}C NMR ($CDCl_3$; at room temperature): δ_C 161.3, 159.3, 159.0, 158.9, 157.8, 155.9 (s × 6, 3,5-pz), 152.9 (d, J = 184 Hz, *o*-py), 139.4 (dt, J = 165 and 6 Hz, *p*-py), 125.7 (dt, J = 167 and 6 Hz, *m*-py), 100.0, 99.2 (d × 2, J = 172 Hz, 4-pz), 20−28 (CHMe$_2$). Anal. Calcd for $C_{38}H_{54}BN_{11}Pd$: C, 58.35; H, 6.96; N, 19.70. Found: C, 58.10; H, 6.83; N, 19.64. **6^{iPr_2}b** was obtained in 50% yield as yellow crystals. ^{1}H NMR ($CDCl_3$; at room temperature): δ_H 9.01 (2H, d, J = 5 Hz, *o*-py), 7.82 (1H, t, J = 8 Hz, *p*-py), 7.36 (2H, t, J = 7 Hz, *m*-py), 3.59, 3.29, 3.20, 3.03, 2.60, 1.89 (1H × 6, sept × 6, J = 7 Hz, C*H*Me$_2$), 1.52−0.57 (36H, m, CH*Me$_2$*). ^{13}C NMR ($CDCl_3$; at room temperature): δ_C 161.1, 159.0, 158.2, 158.1, 157.3, 155.2 (s × 6, 3,5-pz), 153.2 (d, J = 180 Hz, *o*-py), 138.6 (dt, J = 165 and 6 Hz, *p*-py), 125.0 (dt, J = 167 and 7 Hz, *m*-py), 99.3, 98.9, 98.6 (d × 3, J = 171 Hz, 4-pz), 28.0−20.7 (CHMe$_2$). Anal. Calcd for $C_{40.6}H_{61.4}BN_9O_4Pd$ (**6^{iPr_2}b**·0.1hexane): C, 55.91; H, 7.22; N, 14.71. Found: C, 56.06; H, 7.40; N, 14.81. **6^{Me_2}a** was obtained in 73% yield as yellow crystals. ^{1}H NMR ($CDCl_3$; at room temperature): δ_H 9.13 (2H, d, J = 6 Hz, *o*-py), 7.93 (1H, t, J = 8 Hz, *p*-py), 7.47 (2H, t, J = 7 Hz, *m*-py), 2.46, 2.34, 2.33, 2.31, 2.16, 1.50 (3H × 6, s × 6, Me). ^{13}C NMR ($CDCl_3$; at room temperature): δ_C 152.9 (d, J = 185 Hz, *o*-py), 150.6, 148.9, 148.4, 147.4, 146.9, 144.6 (s × 6, 3,5-pz), 139.4 (d, J = 165 Hz, *p*-py), 125.8 (dt, J = 167 and 6 Hz, *m*-py), 108.1, 107.0, 106.7 (d × 2, J = 172 Hz, 4-pz), 14.1, 13.8, 13.6, 13.3, 12.6 (q × 5, J = 127 Hz, Me). Anal. Calcd for $C_{26.2}H_{30.4}BN_{11}Cl_{0.4}Pd$ (**6^{Me_2}a**·0.2CH_2Cl_2): C, 49.89; H, 4.86; N, 24.42. Found: C, 49.70; H, 4.91; N, 24.26.

X-ray Crystallography. Diffraction measurements were made on a Rigaku RAXIS IV imaging plate area detector with Mo Kα radiation (λ = 0.710 69 Å). All the data collections were carried out at −60 °C. Indexing was performed from three oscillation images, which were exposed for 4 min. The crystal-to-detector distance was 110 mm. Data collection parameters were as follows (detector swing angle(deg)/number of oscillation images/exposure time (min)): 4.0/45/30 (**3^{iPr_2}c**·1.74CH_2Cl_2), 3.0/60/15 (**3^{Me_2}b**), 5.0/36/21 (**4^{Me_2}b**), 4.0/45/23.3 (**3^{Me_2}d**), 5.0/36/20 (**6^{iPr_2}a**·CH_2Cl_2), 5.0°/36/50 min (**6^{iPr_2}b**·0.5CH_2Cl_2). Readout was performed with a pixel size of 100 μm × 100 μm.

(18) teXsan; Crystal Structure Analysis Package, version 1.11; Rigaku Corp., Tokyo, Japan, 2000.
(19) *International Tables for X-ray Crystallography*; Kynoch Press: Birmingham, U.K., 1975; Vol. 4.
(20) Higashi, T. Program for Absorption Correction; Rigaku Corp., Tokyo, Japan, 1995.
(21) (a) Sheldrick, G. M. SHELXS-86: Program for Crystal Structure Determination; University of Göttingen, Göttingen, Germany, 1986. (b) Sheldrick, G. M. SHELXL-97: Program for Crystal Structure Refinement; University of Göttingen, Göttingen, Germany, 1997.

Crystallographic data and the results of refinements are summarized in Table 4. The structural analysis was performed on an IRIS O2 computer using the teXsan structure solving program system[18] obtained from Rigaku Corp., Tokyo, Japan. Neutral scattering factors were obtained from the standard source.[19] In the reduction of data, Lorentz and polarization corrections were made. An absorption correction was also made.[20]

The structures were solved by a combination of direct methods (SHELXS-86,[21] SAPI91, SIR92, or MITHRIL90)[22] and Fourier synthesis (DIRDIF94).[23] Least-squares refinements were carried out using SHELXL-97[21] (refined on F^2) linked to teXsan. All the non-hydrogen atoms were refined anisotropically. Riding refinements were applied to the methyl hydrogen atoms of the isopropyl groups (B(H) = B(C)), and the other hydrogen atoms were fixed at the calculated positions. Riding refinements were applied to the methyl hydrogen atoms (B(H) = B(C)). The CH_2Cl_2 solvates, except that associated with **3^{iPr_2}c**, were refined isotropically. H2 (**3^{Me_2}b**) and H0,1,2 atoms (**6^{iPr_2}a**) were refined isotropically.

Acknowledgment. We are grateful to the Ministry of Education, Culture, Sports, Science, and Technology of the Japanese Government for financial support of this research (Grant-in-Aid for Scientific Research: 11228201).

Supporting Information Available: Tables giving crystallographic results. This material is available free of charge via the Internet at http://pubs.acs.org.

OM010448O

(22) (a) SAPI91: Fan, H.-F. Structure Analysis Programs with Intelligent Control; Rigaku Corp., Tokyo, Japan, 1991. (b) SIR92: Altomare, A.; Burla, M. C.; Camalli, M.; Cascarano, M.; Giacovazzo, C.; Guagliardi, A.; Polidori, G. *J. Appl. Crystallogr.* **1994**, *27*, 435. (c) MITHRIL90: Gilmore, C. J. MITHRIL-an Integrated Direct Methods Computer Program; University of Glasgow, Glasgow, U.K., 1990.

(23) Beurskens, P. T.; Admiraal, G.; Beurskens, G.; Bosman, W. P.; Garcia-Granda, S.; Gould, R. O.; Smits, J. M. M.; Smykalla, C. The DIRDIF Program System; Technical Report of the Crystallography Laboratory; University of Nijmegen, Nijmegen, The Netherlands, 1992.